Angular Distribution of 24.0- and 27.2-MeV Neutrons Scattered by Protons

Thomas W. Burrows*
University of Wisconsin, Madison, Wisconsin 53706†
(Received 21 September 1972)

Angular distributions for elastic scattering of neutrons by protons were measured with a counter telescope between 71 and 158° (c.m.) for neutron energies of 24.0 and 27.2 MeV. The angular distributions agreed with the distributions predicted by Hopkins and Breit. The measured anisotropies, $[\sigma(180°)/\sigma(90°)]-1$, were 0.135 ± 0.014 and 0.183 ± 0.015 at 24.0 and 27.2 MeV, respectively.

INTRODUCTION

Groups at Yale and Buffalo[1] and at Livermore[2] have provided phase shift fits to nucleon-nucleon scattering data at energies below the threshold for pion production. However, the fits obtained by these groups differed at low energies. This discrepancy results partly from the large uncertainties in angular distributions of neutrons scattered by protons for neutron energies below 50 MeV. Breit, Lucas, and Tischler[3] have shown that inclusion of a more precise measurement[4] aided in resolving the ambiguities between analyses. MacGregor, Arndt, and Wright[5] have found that by forcing the phase shifts to reproduce Rothenberg's[4] measurement, the low-energy phase shifts were in reasonable agreement with theoretical expectations, with measurements of the deuteron quadrupole moment, and with the Yale and Buffalo phase shifts. There remain, however, inconsistencies in the n-p scattering data, and additional precise measurements of the relative angular distributions should be valuable.

Precise measurements of the angular distribution in the 20- to 30-MeV range should also help to improve neutron flux measurements in this energy range. The uncertainty in the anisotropy of n-p elastic scattering dominates the total uncertainty in counter telescope measurements of neutron flux.[6]

A difficulty in n-p angular-distribution measurements is that different techniques have to be employed for measurements of forward and backward scattering. Counter telescopes have been restricted to measurements in the backward hemisphere because of the difficulties encountered in detecting low-energy protons. With the development of thin solid-state detectors, fast preamplifiers[7] for these detectors, and particle identification techniques, counter telescope measurements may extend into the forward hemisphere to a c.m. scattering angle of about 70°. This overlaps the angular range of measurements of forward hemisphere scattering.

EXPERIMENTAL METHOD

Neutron Source

The measurements were performed with monoenergetic neutrons from the ^{3}H(d, n)^{4}He reaction. The target was a gas cell containing 1.0 atm of tritium behind a molybdenum foil, 3.3×10^{-4} cm thick. The neutron energy spread, full width at half maximum, was 60 to 90 keV.

Counter Telescope

The counter telescope is shown in Fig. 1. The telescope axis could be set at angles to the left and right of the deuteron beam with an accuracy of 0.5°. The radiator wheel had positions for six targets.

The telescope chamber was kept below 0.05 Torr pressure by a mechanical pump. A liquid-nitrogen cold trap prevented contamination of the detector surfaces by pump oil.

The radiator and the aluminum diaphragm, 1.91 cm in diam, defined the angular spread in the counter telescope. The angular spread, half-angle, was 6.2°.

Radiators

The proton radiators in the telescope were polyethylene foils, 22.6 and 67.8 mg/cm^2 thick, with a hydrogen to carbon ratio[8] of 1.98 ± 0.01.

Flexible graphite, 70.4 ± 2.3 mg/cm^2 thick, with a purity[9] of 0.02% was used for background subtraction. The ratios of carbon atoms in the proton radiators to carbon atoms in the graphite were 0.83 ± 0.04 and 0.28 ± 0.01 for the 67.8- and 22.6-mg/cm^2 radiators, respectively.

The radiators were mounted on 0.25-mm-thick platinum sheet. The polyethylene was attached by heating, while the graphite was attached with Eastman 910 adhesive. Care was taken to use as little adhesive as possible to avoid hydrogen contamination. The counter telescope also contained a blank platinum backing.

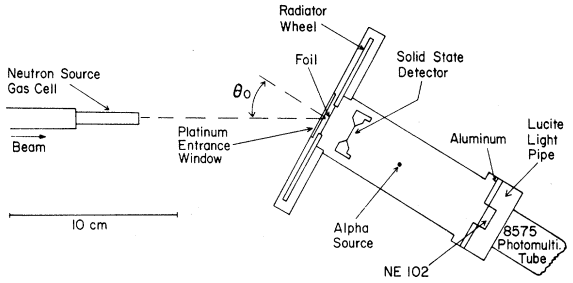

FIG. 1. Counter telescope.

Detectors

The counter telescope contained a silicon surface-barrier transmission detector, 1.0 cm^2 in area, and an NE 102 scintillator, 6.45 cm^2 in area.

The transmission detector[10] was 100 μm thick for experiments with 24.0-MeV neutrons, while for the experiments with 27.2-MeV neutrons, it was 200 μm thick. The resolution of a new detector was less than 50 keV for 5.5-MeV α particles. The detector was replaced when the leakage current had tripled. The NE 102 scintillator was thick enough to stop 30-MeV protons. It was coupled to an RCA 8575 photomultiplier tube.

Electronics

A block diagram of the electronics is shown in Fig. 2. A time-to-amplitude converter (TAC) served as a fast-coincidence circuit with a resolving time of 5 nsec. A window was placed on the TAC peak, and the linear pulses were gated by this single-channel analyzer (SCA). The gated linear signals were fed into an on-line computer where a particle-identification routine analyzed them. The transmission detector spectrum and the TAC spectrum were also monitored on line.

Computer

Initially a particle-identification program, based on the Bethe-Livingston expression[11] for stopping power, provided on-line analysis. This program calculated the particle masses. Two windows, corresponding to two masses, could be set. The energy spectrum of each mass selected was stored.

A second program which calculates the thickness of the transmission detector from a range-energy table[12] was finally used. This program was faster than the initial program and also could identify up to five particles.

The range of a particle with the total energy deposited in both detectors and the range of a parti-

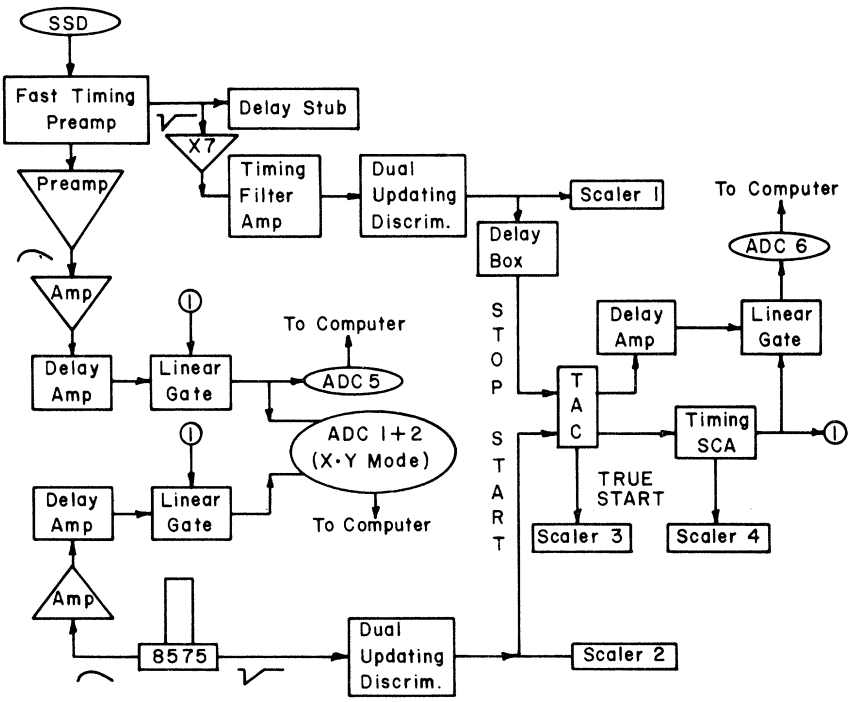

FIG. 2. Block diagram of the electronics.

cle with the energy deposited in the scintillator are extracted from the range-energy table. The difference in the ranges, T, identifies the detected particle. If the detected particle is the one whose range-energy table is stored, T is equal to the actual thickness of the transmission detector. For a different type of particle, T will differ from the detector thickness. Therefore, there will be a peak in the calculated thickness spectrum corresponding to each type of particle. Up to five windows, corresponding to five particles, could be set on the calculated thickness spectrum. For each particle selected, the energy spectrum was stored.

Figure 3(a) shows typical mass spectra obtained with the first program, while typical T spectra are displayed in Fig. 3(b). The apparent low-mass peak below channel 15 in Fig. 3(a) is beam-associated background.

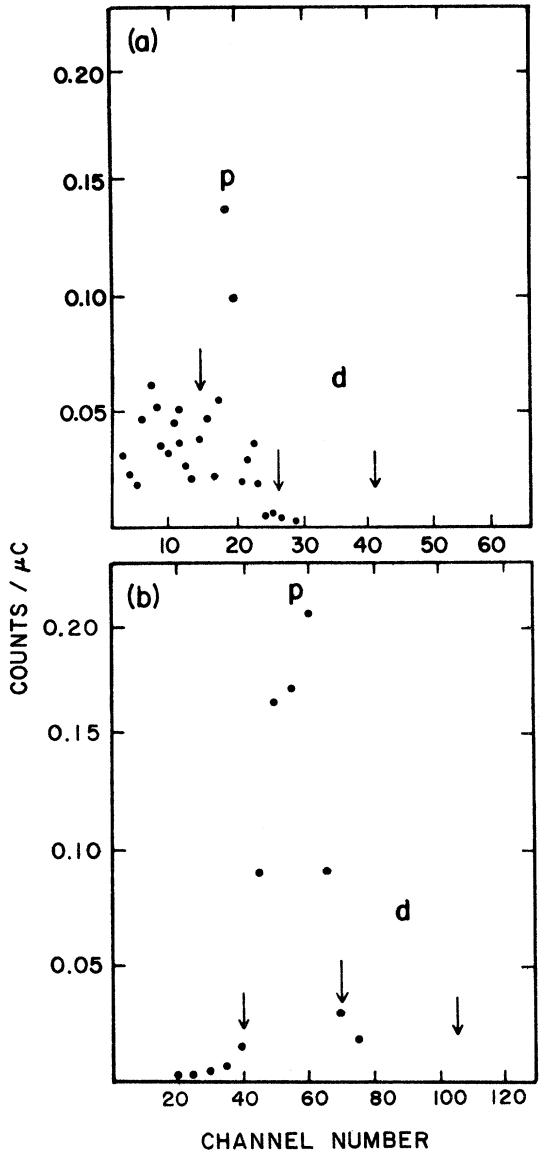

FIG. 3. (a) Typical mass spectrum using the first particle-identification program. (b) Typical front detector thickness spectrum calculated by the second particle-identification program. The triton range-energy table was used. The arrows indicate the cutoff points for protons and deuterons. $E_n = 24.0$ MeV. $\theta_{lab} = 0°$. 22.6-mg/cm^2 polyethylene radiator.

Procedure

Data were taken with the telescope at various angles, both left and right of 0°, up to 53.5° (lab). At each angle spectra were collected with the proton radiator, the carbon subtraction sample, and a blank. None of the pulses with the blank in posi-

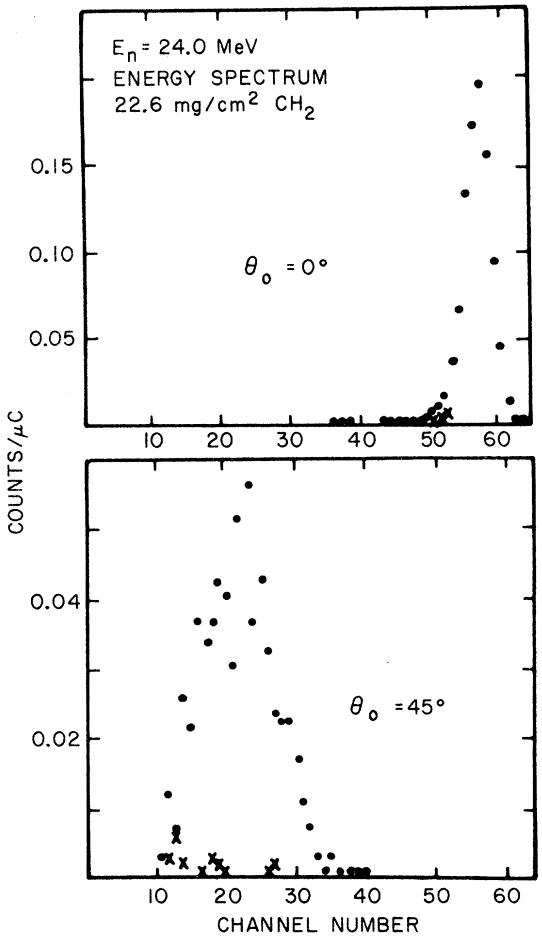

FIG. 4. Typical energy spectra. ●, polyethylene; ×, carbon. The carbon background has been multiplied by the ratio of carbon atoms in the polyethylene to carbon atoms in the background subtraction sample, 0.28.

tion occurred under the proton peak. Chance coincidences were determined by inserting a small delay in one arm of a fast-coincidence circuit. The chance coincidences did not occur under the proton peak and were always less than 3% of foreground. Also, the beam-associated background was observed with the proton radiator in position and no tritium in the gas cell. The beam-associated background was never under the proton peak and was neglected.

The spectra for a given target, detector, and angle, both left and right, were added. Figure 4 displays typical energy spectra. The background was subtracted in two steps. First, the background spectra were compared with the foreground spectra to determine the channels at which foreground and background merged. The proton peaks in the background-corrected energy and mass spectra were integrated. The two values obtained were compared and the limits of integration adjusted until there was good agreement.

RESULTS

The mean laboratory recoil angle, θ_M was obtained from the relationship

$$\cos\theta_M = C(\theta_0)\cos\theta_0, \tag{1}$$

where θ_0 is the setting angle and $C(\theta_0)$ is the correction factor derived by Nakamura[13]:

$$C(\theta_0) = 1 - [(R_1^2 + R_2^2)/L^2 + (R_1/D)^2(0.75 - 2\sin^2\theta_0) + (R_1^2/2LD\cos\theta_0)(1 - 1.5\sin^2\theta_0)]. \tag{2}$$

(See Fig. 5 for the geometry.) For the present measurements $R_1 = 0.95$ cm, $R_2 = 1.27$ cm, $L = 16.2$ cm, and $D = 10.5$ cm. Table I summarizes the results. The finite angles subtended have the largest effect on the mean angle at 0°.

Dead-time effects were less than 0.1% at all angles, and no correction was applied. The correction for the attenuation of the neutrons by inelastic processes in the platinum backing and window amounted to 0.7% in the ratio of $\sigma(158°)/\sigma(71.3°)$.

The effects of Coulomb scattering were estimated as follows: (1) Inscattering compensates outscattering within 0.1%; (2) losses from single scattering were less than 0.2%; and (3) multiple scattering at the edge of the diaphragms increased the effective radii of the diaphragms by less than 0.1%.[14,15] Inelastic scattering of protons in the detectors was less than 0.5%. No corrections for these small effects were applied.

The laboratory count rates were transformed relativistically to a c.m. angular distribution.[16] The c.m. angles and the lab-to-c.m. transformations are summarized in Table I. The data were fitted by the least-squares method to a second-order Legendre polynomial expansion and normalized to the total cross sections calculated by Hopkins and Breit.[17] The fit and normalized differential cross sections, $\sigma(\theta_{c.m.})$ are summarized in Table II. The uncertainties in the differential cross sections include uncertainties in areal den-

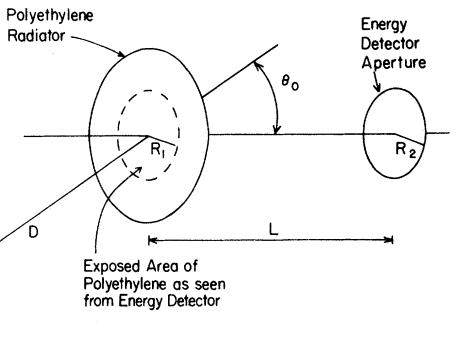

FIG. 5. Geometry of the counter telescope. R_1 is the radius of the exposed portion of the radiator as seen from the energy (E) detector aperture, R_2 is the radius of the E detector aperture, D is the distance from the neutron source to the radiator, L is the distance from the radiator to the E detector aperture, and θ_0 is the angle between the deuteron beam and the telescope axis.

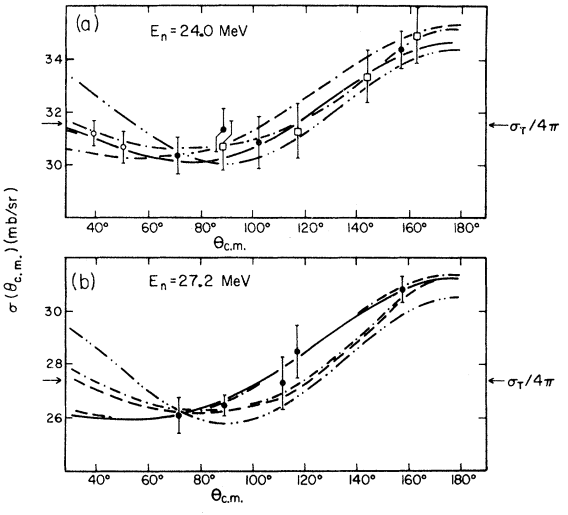

FIG. 6. (a) Angular distribution at $E_n = 24.0$ MeV. The solid line represents the three-parameter fit to the present data and the data of Masterson and Rothenberg. (b) Angular distribution at $E_n = 27.2$ MeV. The solid line represents the three-parameter fit to the present data. The arrows represent the differential cross section for an isotropic distribution: ●, present data; ○, Ref. 8; □, Ref. 4; ---, Hopkins and Breit Yale phase shifts; -·-, Hopkins and Breit LRL 10 phase shifts; -···-, $\sigma_T(1 + B\cos^2\theta)/4\pi(1 + \frac{1}{5}B)$; ·---·, $\sigma_T(1 - \frac{1}{2}B\cos\theta + \frac{1}{2}B\cos^2\theta)/4\pi(1 + \frac{1}{6}B)$. $B = 2(E/90)^2$.

TABLE I. Mean angles, and lab-to-c.m. transformation.

Neutron energy (MeV)	θ_0 (deg)	$C(\theta_0)$	θ_M (deg)	$\theta_{c.m.}$ (deg)	Lab-to-c.m. conversion for $\sigma(\theta_{c.m.})$
24.0	0.0	0.982	11.0	157.9	0.253
	37.5	0.989	38.3	103.0	0.318
	45.0	0.992	45.5	88.7	0.353
	53.5	0.983	54.2	71.3	0.428
27.2	0.0	0.982	11.0	157.8	0.252
	30.0	0.986	31.3	117.0	0.294
	33.0	0.987	34.1	111.4	0.301
	45.0	0.992	45.5	88.6	0.357
	53.5	0.983	54.2	71.2	0.426

sities and compositions, statistics, and the uncertainty in normalization. The total cross sections calculated by Hopkins and Breit are based on the LRL 10 constrained phase shifts.

There are additional uncertainties in the coefficients A_1 and A_2 because of the choice of the second-order Legendre polynomial expansion. For example, the data may be fitted equally well to a distribution of the form $A_0 + A_2 P_2(\cos\theta)$. Such a fit would yield $A_0 = 0.93 \pm 0.01$ and $A_2 = 0.08 \pm 0.01$ at 24.0 MeV and $A_0 = 0.913 \pm 0.006$ and $A_2 = 0.11 \pm 0.01$ at 27.2 MeV. The effect of neglecting higher-order Legendre polynomials may be estimated from the fits to fourth-order Legendre polynomial expansions made by Hopkins and Breit.[17] The uncertainty in A_1 owing to neglecting higher-order terms is 20%, while the uncertainty in A_2 is 10%.

Figure 6(a) shows the present data, the differential cross sections obtained by Masterson,[18] and the angular distribution measured by Rothenberg[4] at 24.0 MeV. Only the differential cross sections measured by Masterson are absolute. Also shown in Fig. 6(a) is a fit to a second-order

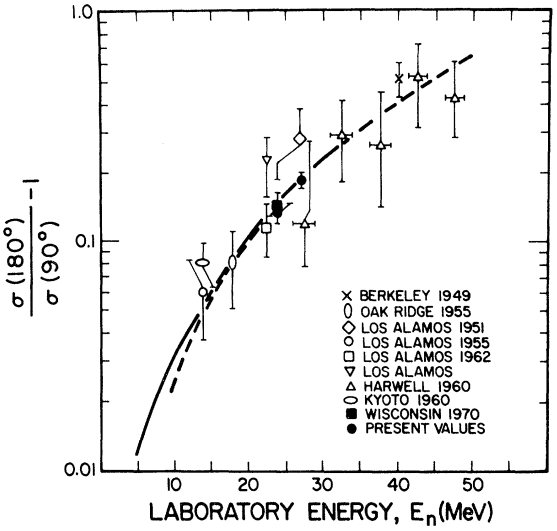

FIG. 7. Measured values of $[\sigma(180°)/\sigma(90°)] - 1$ as a function of neutron energy. The solid line is from Table VII of Ref. 17. The dashed line is the anisotropy suggested by Gammel, $2(E/90)^2$.

Legendre polynomial expansion of the present data at 24.0 MeV and the data obtained by Masterson[18] and Rothenberg.[4] The coefficients of the fit were $A_0 = 31.5 \pm 0.1$ mb/sr, $A_1 = -1.4 \pm 0.2$ mb/sr, and $A_2 = 1.8 \pm 0.3$ mb/sr. Figure 6(b) presents the data and the three-parameter fit at 27.2 MeV. The other curves in Fig. 6(a) and (b) illustrate the cross sections calculated by Hopkins and Breit[17] and those suggested by Gammel.[19] The arrows indicate the differential cross section for an isotropic distribution. All the cross sections, except those derived from the Yale phase shifts, were normalized to the same total cross section.

The rms deviations of the present angular distributions from the relative angular distributions

TABLE II. Summary of data.

Neutron energy (MeV)	$\theta_{c.m.}$ (deg)	$\left\langle \frac{\sigma(\theta_{c.m.})}{\sigma(158°)} \right\rangle_{av}$	$\sigma(\theta_{c.m.})$ (mb/sr)	A_0	A_1	A_2	σ_T [a] (mb)	$\sigma_T/4\pi A_0$ (mb/sr)
24.0	157.9	1.00 ± 0.01	34.4 ± 0.7	0.92 ± 0.02	-0.06 ± 0.04	0.03 ± 0.03	397 ± 4	34.4 ± 0.7
	103.0	0.90 ± 0.03	31.0 ± 1.2					
	88.7	0.91 ± 0.02	31.4 ± 0.8					
	71.3	0.88 ± 0.02	30.4 ± 0.7					
27.2	157.8	1.00 ± 0.01	30.8 ± 0.5	0.889 ± 0.005	-0.08 ± 0.01	0.05 ± 0.01	344 ± 3	30.8 ± 0.4
	117.0	0.92 ± 0.03	28.3 ± 1.0					
	111.4	0.89 ± 0.04	27.4 ± 1.3					
	88.6	0.86 ± 0.01	26.6 ± 0.4					
	71.3	0.85 ± 0.02	26.1 ± 0.7					

[a] The total cross section σ_T was interpolated from Table VII of Ref. 17.

calculated from Tables VI and VII of Hopkins and Breit[17] are 1.4% for the Yale phase shifts and 1.5% for the LRL 10 constrained phase shifts. These deviations are consistent with the 1.5% mean uncertainty of the data. The rms deviation from the symmetric distribution, $1+2(E/90)^2\cos^2\theta$, suggested by Gammel[19] is 1.7%.

Figure 7 summarizes the measured values of the anisotropies, $[\sigma(180°)/\sigma(90°)-1]$, in the 10- to 50-MeV range. The points shown were measured at Los Alamos in 1951,[20] 1955,[21] 1962,[22] and later,[23] at Oak Ridge,[24] at Kyoto,[13] at Berkeley,[25] at Harwell,[26] and at Wisconsin.[4] Most of these points were obtained from angular distributions fitted to $A(1+B\cos^2\theta)$, a distribution suggested by Gammel[19] as a phenomenological fit to the data available in 1957 from 14 to 90 MeV. The present values at 24.0 and 27.2 MeV were obtained from the fits to a two-parameter symmetric distribution, $A_0+A_2P_2(\cos\theta)$. The anisotropies were 0.135 ± 0.014 and 0.183 ± 0.015 at 24.0 and 27.2 MeV, respectively. The weighted mean of the present value at 24.0 MeV and Rothenberg's[4] measurement is 0.139 ± 0.011. The dashed curve is the Gammel[19] suggestion, $2(E/90)^2$, while the solid curve is from Table VII of Hopkins and Breit.[17]

It is not surprising that there should be good agreement between the present and Rothenberg's[4] measurements and the LRL 10 constrained phase shift calculations, since MacGregor, Arndt, and Wright[5] forced the phase shifts to reproduce Rothenberg's measurement. MacGregor, Arndt, and Wright found, however, that if the phase shifts are not constrained, the calculated anisotropy at 24 MeV is 0.08. This value is 40% lower than the present measurement and Rothenberg's measurement.

ACKNOWLEDGMENTS

I thank Professor H. H. Barschall for suggesting this experiment. Many helpful discussions and aid in the experiment from Dr. L. N. Rothenberg, Dr. D. Hilscher, Dr. J. C. Davis, Dr. T. G. Masterson, Professor P. A. Quin, and F. T. Noda are gratefully acknowledged. I am also grateful to Dr. S. E. Vigdor for developing the second particle-identification program used.

---

* Now at University of Kentucky, Lexington, Kentucky.

† Work supported in part by the U. S. Atomic Energy Commission.

[1]G. Breit and R. D. Haraez, in *High Energy Physics*, edited by E. H. S. Burhop (Academic, New York, 1967), Vol. 1, p. 21.

[2]M. H. MacGregor, R. A. Arndt, and R. M. Wright, Phys. Rev. 173, 1272 (1968).

[3]G. Breit, J. Lucas, and M. Tischler, Phys. Rev. 184, 1668 (1969).

[4]L. N. Rothenberg, Phys. Rev. C 1, 1226 (1970); and Ph. D. thesis, University of Wisconsin, Madison, Wis., 1969 (unpublished).

[5]M. H. MacGregor, R. A. Arndt, and R. M. Wright, Phys. Rev. 182, 1714 (1969).

[6]J. C. Hopkins, Los Alamos Scientific Laboratory Report No. LA-DC-8791, 1967 (unpublished).

[7]I. S. Sherman, R. G. Roddick, and A. J. Metz, IEEE Trans. Nucl. Sci. 15, (No. 3), 500 (1968).

[8]Galbraith Laboratories, Knoxville, Tenn.

[9]Poco Graphite, Inc., Decatur, Texas.

[10]EDAX, Inc., Prairie View, Ill.

[11]M. S. Livingston and H. A. Bethe, Rev. Mod. Phys. 9, 245 (1937).

[12]B. Hird and R. W. Ollerhead, Nucl. Instr. Methods 71, 231 (1969).

[13]T. Nakamura, J. Phys. Soc. Japan 15, 1359 (1960).

[14]R. M. Sternheimer, Rev. Sci. Instr. 25, 1070 (1954).

[15]E. D. Courant, Rev. Sci. Instr. 22, 1003 (1951).

[16]R. E. Phillips and S. T. Thornton, Oak Ridge National Laboratory Report No. ORNL-4179, 1967 (unpublished).

[17]J. C. Hopkins and G. Breit, Nucl. Data A9, 137 (1971).

[18]T. G. Masterson, Ph.D. thesis, University of Wisconsin, Madison, Wis., 1971 (unpublished); Phys. Rev. C 6, 690 (1972).

[19]J. L. Gammel, in *Fast Neutron Physics*, edited by J. B. Marion and J. L. Fowler (Interscience, New York, 1963), Pt. II, p. 2185.

[20]J. E. Brolley, Jr., J. H. Coon, and J. L. Fowler, Phys. Rev. 82, 190 (1951).

[21]J. D. Seagrave, Phys. Rev. 97, 757 (1955).

[22]E. R. Flynn and P. J. Bendt, Phys. Rev. 128, 1268 (1962).

[23]W. Leland, J. Beery, H. Bryant, and E. Flynn, private communication as quoted in Ref. 6.

[24]A. Galonsky and J. P. Judish, Phys. Rev. 100, 121 (1955).

[25]J. Hadley, E. Kelly, C. Leith, E. Segrè, C. Wiegand, and H. York, Phys. Rev. 75, 351 (1949).

[26]J. P. Scanlon, G. H. Stafford, J. J. Thresher, P. H. Bower, and A. Langsford, Nucl. Phys. 41, 401 (1963).